# UPGRADE OF KEK ELECTRON/POSITRON INJECTOR LINAC USING PULSED MAGNETS AND MACHINE LEARNING

T. Natsui†, T. Kamitani, K. Yokoyama, Y. Okayasu, M. Satoh, D. Wang
KEK, Ibaraki, Japan

*Abstract*

The KEK injector linac injects high-charge electron and positron beams into the high-energy ring and low-energy ring of SuperKEKB, respectively. The linac also injects electron beams into two light source rings: the PF ring and the PF-AR. We operate simultaneous top-up injections into the four rings using many pulsed magnets. We upgraded the linac to attain higher-quality beam injections for SuperKEKB rings. In the summer of 2023, large-aperture pulsed quadrupole magnets were installed upstream of the linac and driven by large-current pulse power supplies with markedly high electric efficiency. These new magnets changed the pulse-by-pulse optics to provide high-quality beams. To manage complex beam injections into the four rings, we introduced an automatic adjustment system using machine learning. The system surpassed human skills in beam adjustment and resulted in significant increases in the amount of beam charge and transmission.

## INTRODUCTION

The KEK has four storage rings for the electron/positron collider rings and two light source rings. The collider rings include the high-energy ring (HER) and low-energy ring (LER), which are the SuperKEKB main rings [1]. The PF ring and PF-AR are the light source rings. Figure 1 shows a schematic of the KEK electron/positron injector linac. The linac is a 50 pps pulse operation. We have already achieved a simultaneous four-ring top-up injection. We use two types of electron guns: a photocathode RF gun and a thermionic DC gun. The RF gun generate the HER low-emittance electron beam. The required emittances were 40 and 20 mm-mrad in horizontal and vertical directions, respectively. In contrast, the DC gun for the positron primary electron beam had a high charge of 10 nC per bunch. The DC gun is also used for the light source rings (PF and PF-AR). In sector 1, a positron target is installed in front of a flux concentrator (FC) [2]. Positrons are generated by colliding a 10 nC primary electron with a tungsten target. In the positron capture section, Large-Aperture S-band (LAS) accelerator structures were used. In addition, we have a damping ring for the positron beam. The damping ring is located between sectors 2 and 3 of the injector linac. Table 1 lists the injection beam specifications for each ring. As the requirements of the beams differed, we have to change the linac acceleration conditions. We achieved the simultaneous top-up injection of four rings using two types of electron guns and several pulsed magnets [3].

Further, we had to accelerate various beams with different parameters on a single beamline. Thus, pulsed magnets were used for all quadrupole magnets (Q magnets) and steering magnets in sectors 3 to 5 [4]. These pulsed magnets were introduced in 2017 and allowing optics changes every 20 ms. In 2023, large-aperture pulsed Q magnets were also introduced for optics matching around the 180° bending section of the J-arc. This was advantageous for transmitting a highly charged positron primary beam to the target without loss.

Table 1: Specifications of Each Beam

| **Ring** | **Beam** | **Energy** | **Charge** |
|---|---|---|---|
| HER | Electron | 7.0 GeV | 4.0 nC |
| LER | Positron | 4.0 GeV | 4.0 nC |
| PF ring | Electron | 2.5 GeV | 0.3 nC |
| PF-AR | Electron | 6.5 or 5 GeV | 0.3 nC |

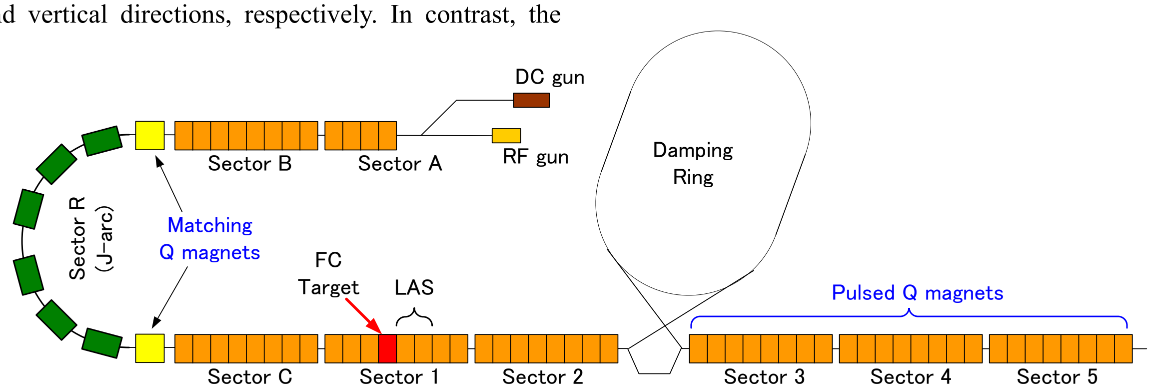


Figure 1: KEK injector linac consisting of eight acceleration sectors and a 180° bending sector (J-arc). Sectors 3 to 5 have pulsed Q magnets and pulsed steering magnets. The new large-aperture Q magnets were installed at J-arc in the summer of 2023 to match each beam mode.

†takuya.natsui@kek.jp

A large-aperture pulsed Q magnet requires a high-power pulse driver. We developed a new high-power pulse driver for these new pulsed magnets. The introduction of pulsed magnets provided many degrees of freedom for tuning each beam mode; however, it also increased the time and effort required for beam tuning. Therefore, we introduced automatic tuning using machine learning. We established an automatic tuning method using Bayesian optimization and developed flexible tuning software for various purposes. The next sections present the large-diameter Q magnets and the results of automatic tuning.

## PULSED Q MAGNET UPGRADE

In sectors 3‐5, all Q magnets were pulsed. Downstream of the damping ring, the transverse beam sizes were small in all modes; therefore, a pulsed Q magnet with a 20 mm aperture could be used. These small-aperture magnets were referred to as PM_32_4 type. The inductance of the Q magnet was 1.0 mH, and the maximum pulse current was 330 A. The pulse driver raises a current within 3 ms at a voltage of 220 V. However, these pulsed Q magnets and pulse drivers could not be used upstream of the injector because of the large positron primary beam size. In the bending sector (J-arc), the beams could not be independently matched because the Q magnets were DC magnets.

### *Large-aperture Pulsed Q magnet*

We replaced the DC Q magnets at the entrance and exit of the J-arc with pulsed Q magnets. The positron beam was prone to charge loss because of its large beam size and wide energy spread in the J-arc. Beam matching at the J-arc is also important for HER electron beams, because an unexpectedly large β (Twiss parameter) creates transverse wake fields that worsen the emittance. The Twiss parameter mismatch makes it difficult to adjust the electron beam, which must pass through a small hole adjacent to the positron generation target. Installing a pulsed Q magnet in the matching section is useful for beam tuning. Large-aperture magnets are required for a large beam size of the J-arc. As the existing pulsed Q magnet (PM_32_4 type) had a narrow aperture, a new large-aperture Q magnet was installed. This Q magnet was called the PM_R0_01 type. Table 2 lists the specifications of the pulsed Q magnet. The new PM_R0_01 type had an aperture that was more than twice that of the old type. Figure 2 shows a photograph of the PM_R0_01 type Q magnet. Figure 3 shows a view of the J-arc with pulsed Q magnets in place.

Generally, the current of a Q magnet is proportional to the square of its bore diameter. Therefore, an existing pulse driver could not be used for this new large-aperture pulsed Q magnet, and a high-power driver had to be developed. The PM_R0_01 type Q magnet was designed such that its inductance was close to that of the existing magnets. As shown in Table 2, the new magnet requires approximately twice the current and voltage of the existing magnet. Therefore, developing a pulse driver with nearly four times the power of the existing driver was necessary.

Table 2: Specifications of the Q Magnet

| | **PM_32_4** | **PM_R0_01** |
|---|---|---|
| L@ 1 kHz | 1.0 mH | 1.28 mH |
| Max. Current | 330 A | 600 A |
| Gap | ϕ 20 mm | ϕ 44 mm |
| Length | 200 mm | 300 mm |
| Magnetic field | 60 T/m | 20 T/m |

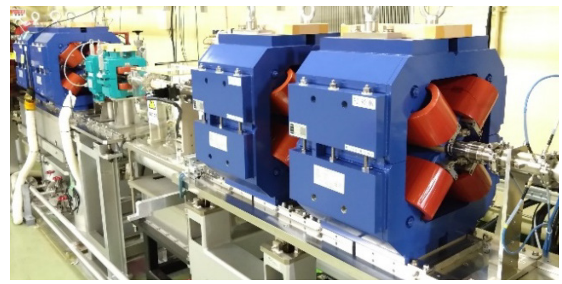

Figure 2: Photo of new pulsed Q magnet.

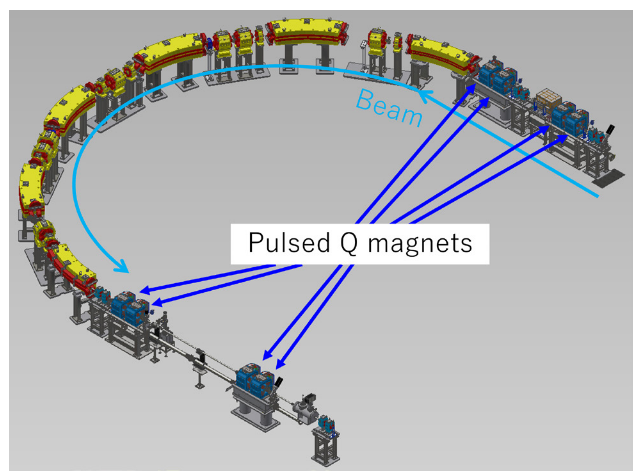


Figure 3: Pulsed Q magnets in J-arc.

### *High-power Pulse Driver*

The inductance of the drive magnet was 1.28 mH, and we intended to increase the current to 600 A within 3 ms; therefore, a voltage of 400 V was applied to the magnet. The circuit configuration was straightforward and consisted of a capacitor (14 mF), charger (400 V), and H-bridge circuit, as shown in Fig. 4. The H-bridge had two diodes and two insulated gate bipolar transistors (IGBTs) as switches. The current amplitude was adjusted by controlling the switching timing of the two IGBTs, and energy recovery was performed [5]. This circuit could recover the magnetic field energy stored in the magnet.

The magnetic energy was 2.3 J at 600 A ($W = L I^2/2$). If energy recovery was not used, the power consumption was 10 kW at 50 pps. Energy recovery was important to achieve power savings and easy cooling.

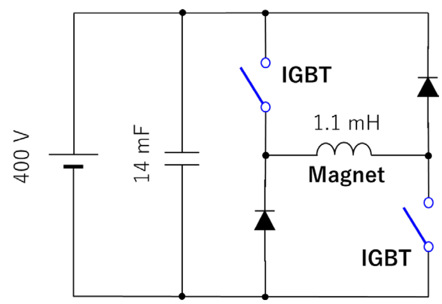


Figure 4: Circuit configuration of pulse driver.

Driver devices with sufficient current and voltage margins were selected. A general-purpose power supply was used as the charger. The driver was divided into a capacitor and an IGBT housing. Each chassis was a 4U 19-inch rack. The driver contained an electronic circuit that received an external trigger and generated an isolated trigger for the IGBTs. The driver was controlled by an external trigger. The magnet current was controlled using the trigger pulse width. As the trigger timing and pulse width depended on the required current, a calculated control signal was provided to the driver. Figure 5 shows the relationship between the trigger pulse and magnet current.

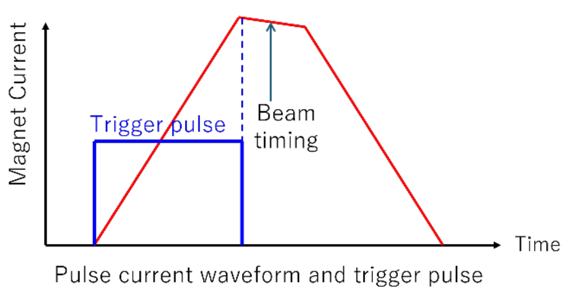


Figure 5: Control trigger pulse and current waveform of pulse deriver.

Figure 6 shows the current waveform of the driver with a pulsed Q magnet as the load. The point t = 0 on the x-axis of the graph represents the beam timing. The graph shows the results for different trigger pulse widths. With a pulse of approximately 2.5 ms, a current of 600 A could be applied, and a 50 pps operation has been successfully achieved. An energy recovery efficiency of greater than 80 % was achieved. The drivers have been in operation since the autumn of 2023 and were sufficiently stable to be used under actual operating conditions with pulse-to-pulse current change operation. Individual beam matching is now possible in the J-arc, which is particularly helpful in reducing the loss of positron primary beams.

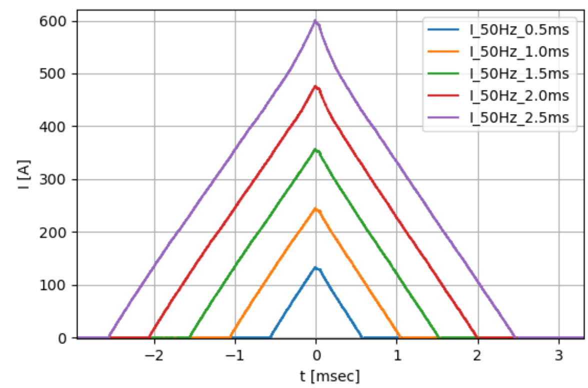


Figure 6: Current waveform.

## AUTOMATIC TUNING WITH ML

The injector had many pulsed magnets and varied the beam optics pulse-to-pulse to achieve simultaneous top-up injection into the four rings. The RF phase also changed pulse-to-pulse to match the energy of each ring. In recent years, as the number of pulsed magnets increased, the number of tuning parameters also increased, and the quality of the beam improved accordingly. However, the difficulty and time required for tuning have increased. Therefore, we introduce an automatic tuning tool using machine learning. Previously, experienced operators had to spend a lot of time tuning the beam; however, with the introduction of automatic beam tuning, anyone could tune the beam to a certain quality in a short time. In several examples, automatic tuning using machine learning has outperformed humans.

### *Principle and Method*

Machine tuning is the process of changing the tuning parameters to improve the output. For example, the current of the magnet can be changed to bring the beam orbit closer to its center. Usually, several tuning knobs exist as magnet current values or RF phases of accelerating structures. Defining what constitutes a "good state" is also necessary depending on the purpose. In any case, a good state is defined when a certain scalar value is defined from single or multiple monitor values and that value is at its minimum or maximum. Thus, converting machine tuning into a problem of minimizing an unknown multivariate function is required. Bayesian optimization [6] can be used to solve minimization problems for unknown functions. This method uses a Gaussian process to predict the function and its variance, from which the next search point is derived. This method is highly efficient in obtaining the optimal point, making it suitable for practical machines with a limited number of measurements [7]. The downhill simplex method (Nelder-Mead method) is a classical method for solving unknown function minimization problems [8] and a simple algorithm; if the function is smooth, it reliably converges to a minimum point. However, if the shape of the function is complex, it may become a local minimum. Bayesian optimization is effective when the beam tuning is poor and a wide area must be searched. The downhill simplex is effective when the optimal point is nearby, such as when the beam condition shifts slightly from a good state owing to instrument drift.

## *Implementation*

All KEK injector linac instruments are controlled using EPICS. The adjustment knobs and measurement items varied depending on the purpose of tuning. EPICS is compatible with auto-tuning tools because it allows various devices to be controlled from the same interface. Python was used for software implementation, including the GUI. A Python library called GPyOpt was used for Bayesian optimization [9]. The downhill simplex method was coded from scratch.

The actual operating panel and its description are shown in Fig. 7. In this panel, the EPICS recode can be selected as control items (X setting) and monitor items (Y setting). The control item allowed the tuning range to be selected. The value obtained from the monitored item was used to define the evaluation value, and automatic tuning was performed to minimize the evaluation value. The tuning algorithm is selectable between Bayesian optimization and downhill simplex. Normally, an operator can simply load a preproduced setting file and execute it for automatic tuning.

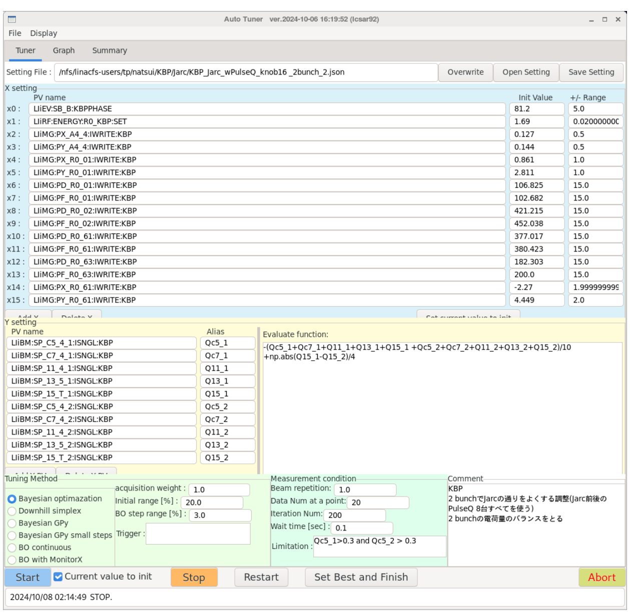

Figure 7: Automatic tuning panel.

## *Practical Examples*

An example is the initial parameter search for positron generation. At machine start-up, the primary beam did not hit the target well, and the position generation rate was low. If the primary beam has a certain amount of transmission, the positron beam generation rate can be increased by tuning the upstream beamline. Typically, subharmonic bunchers (SHB) and several upstream pulsed steering magnets are adjusted. We have two SHBs. The following are the results of the automatic tuning with Bayesian optimization using six tuning knobs (two SHB phases and four steering magnet currents). Figure 8 shows a time-series graph during the tuning. The number of iterations was 50, and in this case, the tuning required 10 min. Figure 9 shows the panel for checking the tuning during the actual operation. This panel allows the user to check the status of the tuning parameter changes (upper graph) and evaluation value updates (lower graph) in real time. Usually, 50 iterations were sufficient to tune the eight or fewer parameters. If the number of parameters exceeded 10, we tuned over approximately 100 iterations.

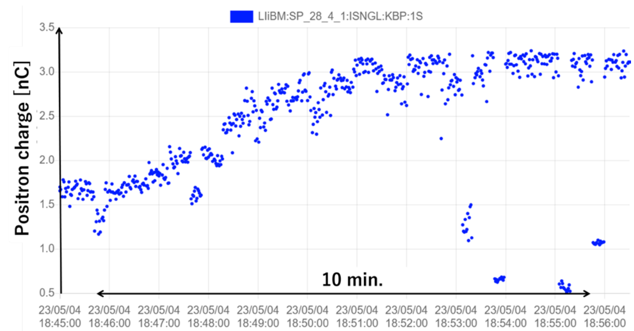


Figure 8: Graph of positron beam charge increase during tuning; tuning was completed in approximately10 min.

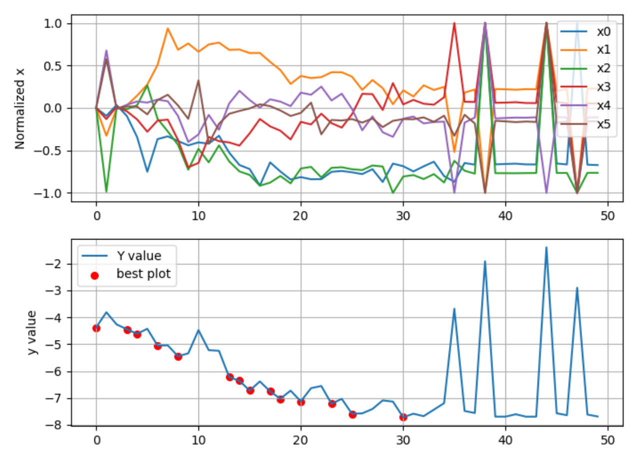


Figure 9: Panel for checking tuning in actual operation. The upper graph is the status of tuning parameter changes. The lower graph is the status of evaluation value updates.

The next example shows the significant contribution to the increase in the charge of the positron beam. The positron beam loss in the acceleration line from the capture section to the damping ring was simulated and predicted to be only approximately 10 %. However, the actual beam loss was approximately 40 % higher than that obtained in the simulation. The positron beam charge did not reach the target value of 4.0 nC and remained at approximately 3.0 nC. The positron beam had a large emittance upstream of the damping ring, and the beam profile was approximately the same as the aperture of the accelerating structure. Therefore, a small orbital or focusing error could easily cause beam loss. In addition, many Q magnets were installed in this section to maintain a small beam size. The number of tuning parameters for these magnets was approximately 200. Furthermore, because the magnets in this section are DC magnets, other beam modes are affected, long study period is not possible.

Therefore, automatic beam tuning was performed in this area to achieve effective beam tuning within a short period of time. However, too many parameters existed to adjust all magnets simultaneously; therefore, the tuning was divided into several sections. In practice, the section was divided into 16 sections and tuned such that the transmittance increased from upstream. The series of tunings from upstream to downstream required approximately 5 h. As a result of this series of tuning, the charge increased from 3.3 nC to 4.0 nC. Figure 10 shows a graph of the BPM monitors. Before tuning, a gradual loss of positron charge occurred; however, after tuning, the loss was reduced. Thus, machine learning enables the adjustment of many parameters in a short time. This is an example of automatic tuning using machine learning that goes beyond human capabilities.

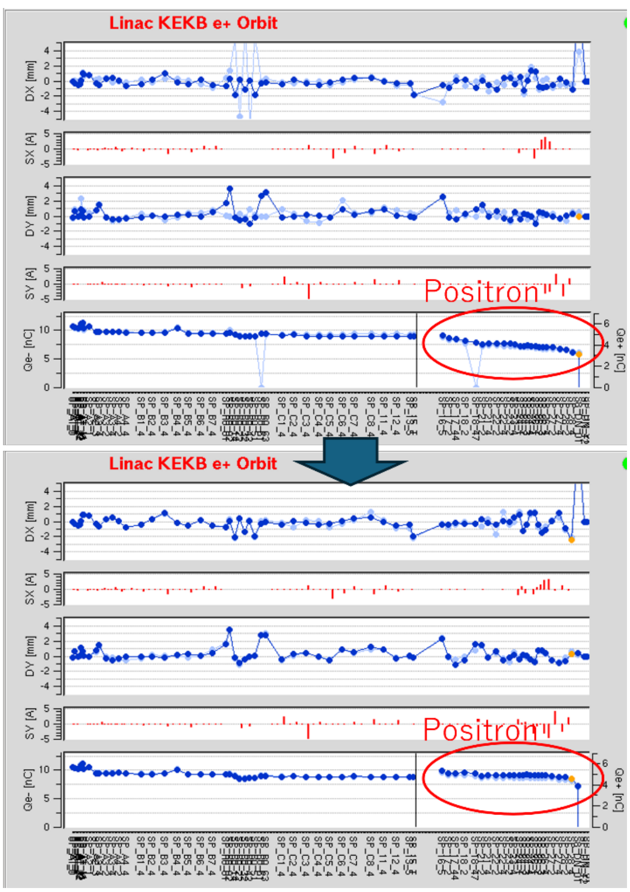


Figure 10: Tuning result of positron capture section tuning. Upper graphs are before tuning. Lower graphs are after tuning.

## SUMMARY

The KEK injector linac has a large number of pulsed magnets, which are useful for adjusting individual beams for different beam modes. Specifically, the newly introduced large-aperture pulsed Q magnet contributes to an increase in the beam charge. The use of a pulsed magnet makes it possible to change the optics in pulse-to-pulse mode and achieve simultaneous four-ring top-up injections. However, increasing the tuning freedom leads to complex operations. Therefore, we introduced an automatic adjustment using machine learning to reduce the adjustment time and manpower. Automatic tuning based on Bayesian optimization can be used in a variety of applications. In particular, it exceeds the expectations for increasing the charge of the positron beams. Thus, we achieved significant upgrades in both the hardware and software, resulting in improved beam quality.

## REFERENCES


[1] Y. Funakoshi *et al.*, “The SuperKEKB Has Broken the World Record of the Luminosity”, in *Proc. IPAC'22*, Bangkok, Thailand, Jun. 2022, pp. 1–5. doi:10.18429/JACoW-IPAC2022-MOPLXGD1

[2] Y. Enomoto, K. Abe, N. Okada, and T. Takatomi, “A New Flux Concentrator Made of Cu Alloy for the SuperKEKB Positron Source”, in *Proc. IPAC'21*, Campinas, Brazil, May 2021, pp. 2954–2956. doi:10.18429/JACoW-IPAC2021-WEPAB144

[3] T. Natsui et al., “KEK e$^+$/e$^-$ Injector Linac”, in *Proc. 65th ICFA Adv. Beam Dyn. Workshop High Luminosity Circular e+e- Colliders (eeFACT'22)*, Frascati, Italy, Sep. 2022, pp. 251-255. doi:10.18429/JACoW-eeFACT2022-THYAT0102

[4] Y. Enomoto *et al.*, “Pulse-to-pulse Beam Modulation for 4 Storage Rings with 64 Pulsed Magnets”, in *Proc. LINAC'18*, Beijing, China, Sep. 2018, pp. 609-614. doi:10.18429/JACoW-LINAC2018-WE1A06

[5] T. Natsui, "Development of new pulse driver for high power pulsed magnet", in *Proc. LINAC2024*, Chicago, IL, USA, Aug. 2024, pp. 418-420. doi:10.18429/JACoW-LINAC2024-TUPB038

[6] R. Garnett, Bayesian Optimization. Cambridge University Press, 2023.

[7] R. Roussel *et al.*, “Bayesian optimization algorithms for accelerator physics,” *Phys. Rev. Accel. Beams*, vol. 27, no. 8, Aug. 2024. doi:10.1103/physrevaccelbeams.27.084801

[8] J. A. Nelder and R. Mead, “A Simplex Method for Function Minimization,” *The Computer Journal*, vol. 7, no. 4, pp. 308–313, Jan. 1965. doi:10.1093/comjnl/7.4.308

[9] https://sheffieldml.github.io/GPyOpt/